Figure S1

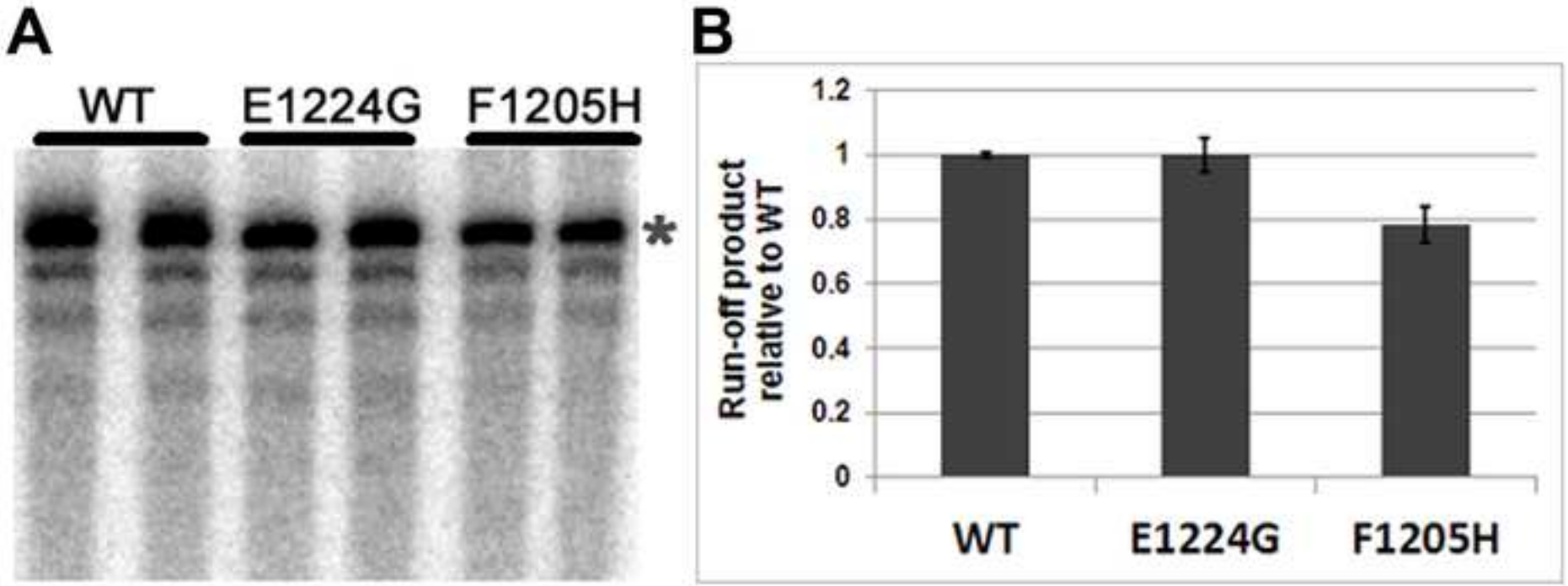
A
WT
E1224G
F1205H
*
B
Run-off product relative to WT
1.2
1
0.8
0.6
0.4
0.2
0
WT
E1224G
F1205H

Figure S2

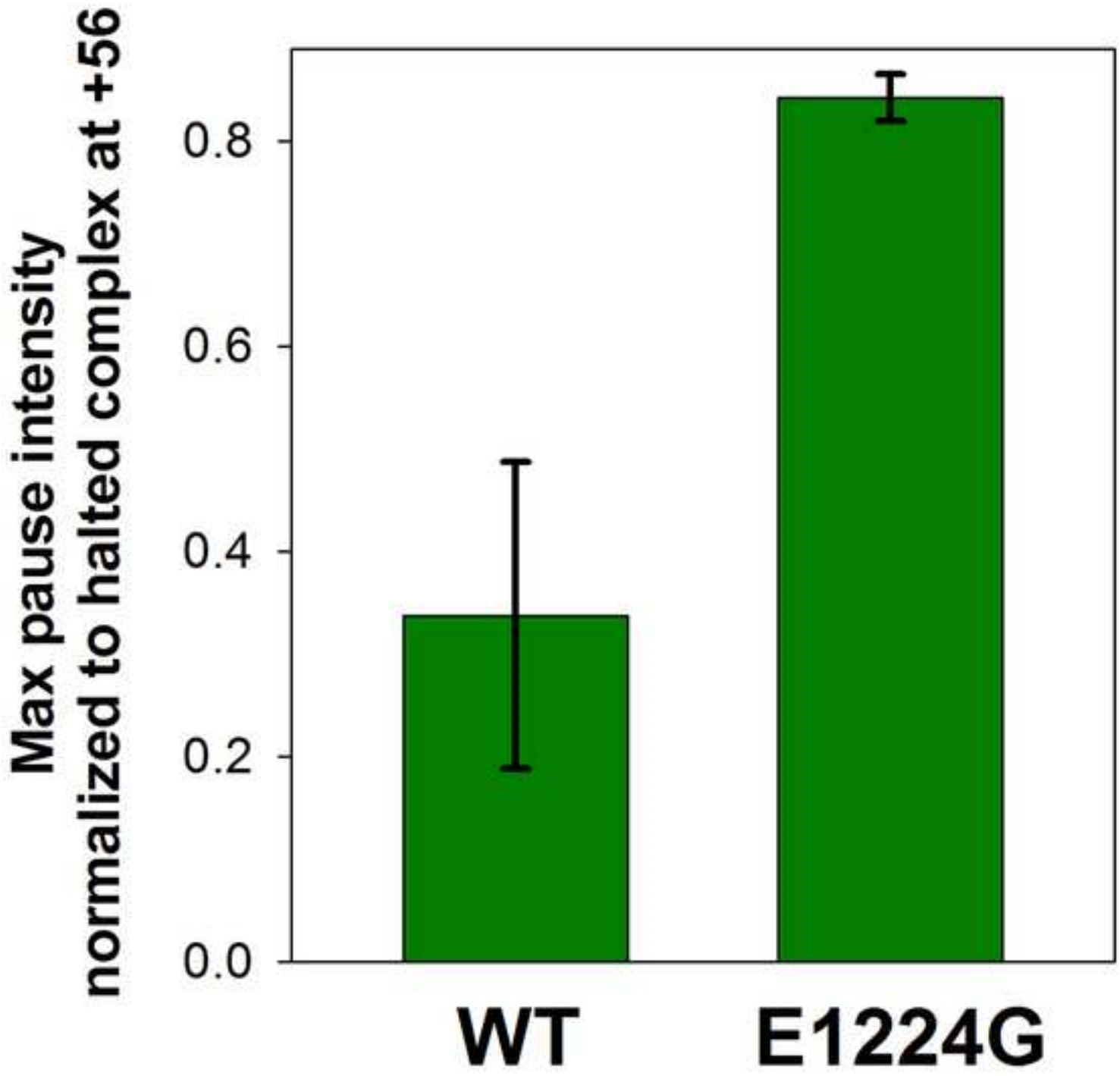
Max pause intensity
normalized to halted complex at +56
0.0
0.2
0.4
0.6
0.8
WT
E1224G

Figure S3

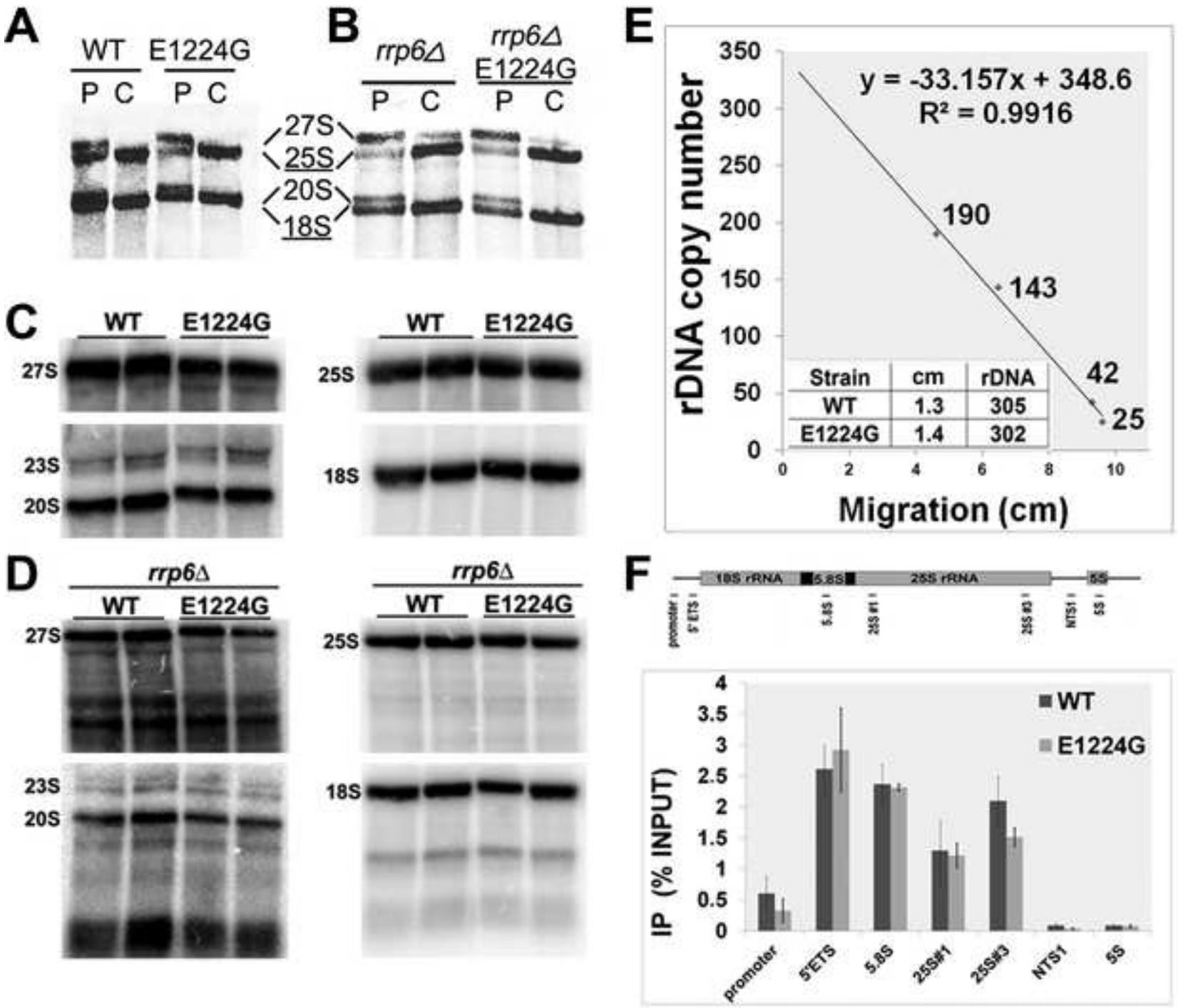
A
WT
E1224G
P C P C
27S
25S
20S
18S
B
rrp6Δ
rrp6Δ
E1224G
P C P C
C
WT
E1224G
27S
23S
20S
25S
18S
D
rrp6Δ
WT
E1224G
27S
23S
20S
25S
18S
E
rDNA copy number
y = -33.157x + 348.6
R² = 0.9916
190
143
42
25
Strain | cm | rDNA
WT | 1.3 | 305
E1224G | 1.4 | 302
Migration (cm)
F
18S rRNA
5.8S
25S rRNA
5S
promoter
5'ETS
5.8S
25S #1
25S #3
NTS1
5S
IP (% INPUT)
WT
E1224G
promoter
5'ETS
5.8S
25S#1
25S#3
NTS1
5S

Figure S4

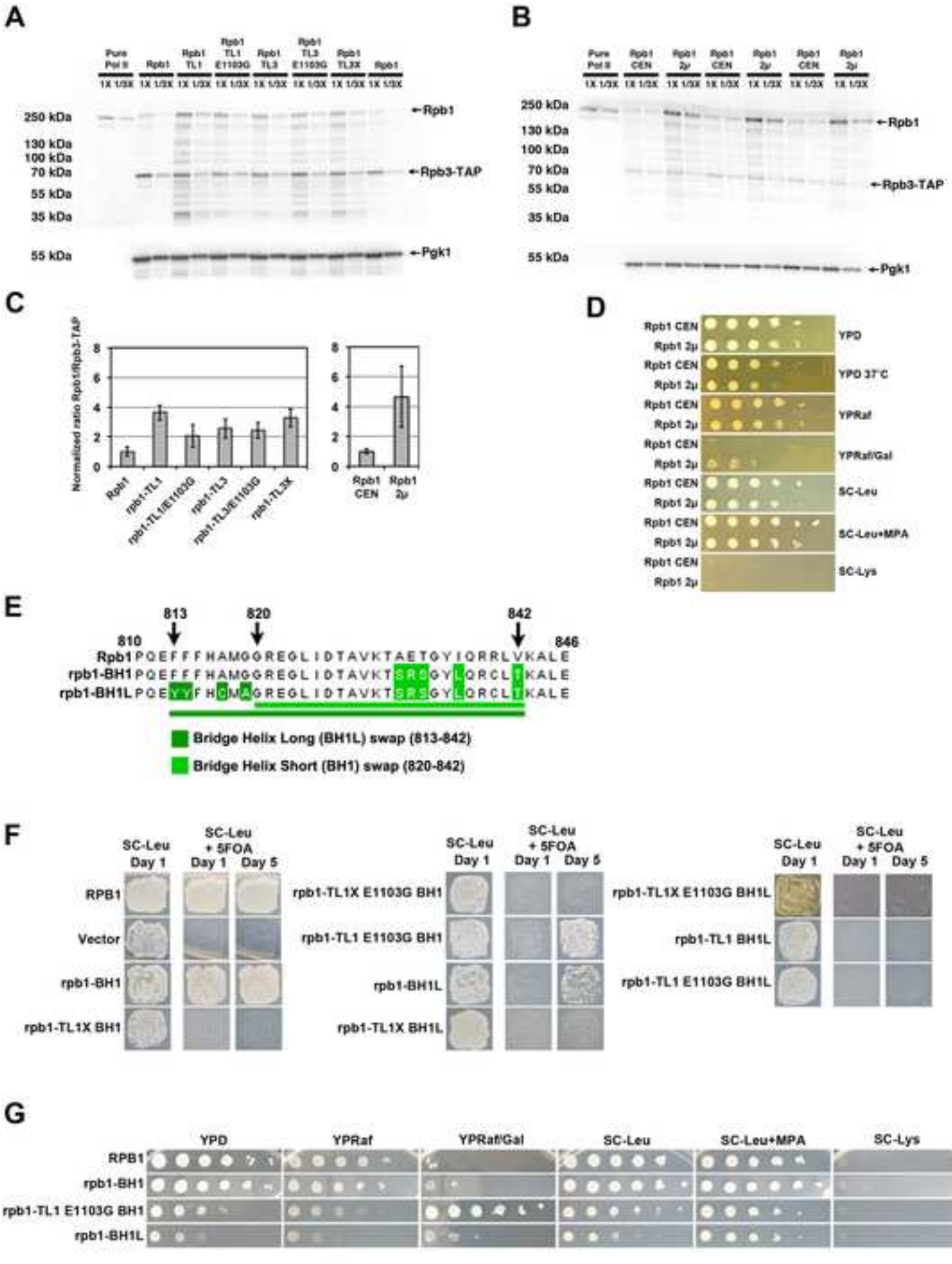
A
Pure Pol II
Rpb1
Rpb1 TL1
Rpb1 TL1 E1103G
Rpb1 TL3
Rpb1 TL3 E1103G
Rpb1 TL3X
Rpb1
1X 1/3X
250 kDa
130 kDa
100 kDa
70 kDa
55 kDa
35 kDa
55 kDa
←Rpb1
←Rpb3-TAP
←Pgk1
B
Pure Pol II
Rpb1 CEN
Rpb1 2μ
Rpb1 CEN
Rpb1 2μ
Rpb1 CEN
Rpb1 2μ
1X 1/3X
250 kDa
130 kDa
100 kDa
70 kDa
55 kDa
35 kDa
55 kDa
←Rpb1
←Rpb3-TAP
←Pgk1
C
Normalized ratio Rpb1/Rpb3-TAP
Rpb1
rpb1-TL1
rpb1-TL1/E1103G
rpb1-TL3
rpb1-TL3/E1103G
rpb1-TL3X
Rpb1 CEN
Rpb1 2μ
D
Rpb1 CEN
Rpb1 2μ
YPD
YPD 37°C
YPRaf
YPRaf/Gal
SC-Leu
SC-Leu+MPA
SC-Lys
E
813
820
842
810
846
Rpb1 PQEFFFHAMGGREGLIDTAVKTAETGYIQRRLVKALE
rpb1-BH1 PQEFFFHAMGGREGLIDTAVKTSRSGYLQRCLTKALE
rpb1-BH1L PQEYYFHGMAGREGLIDTAVKTSRSGYLQRCLTKALE
Bridge Helix Long (BH1L) swap (813-842)
Bridge Helix Short (BH1) swap (820-842)
F
SC-Leu Day 1
SC-Leu + 5FOA Day 1
Day 5
RPB1
Vector
rpb1-BH1
rpb1-TL1X BH1
rpb1-TL1X E1103G BH1
rpb1-TL1 E1103G BH1
rpb1-BH1L
rpb1-TL1X BH1L
rpb1-TL1 BH1L
rpb1-TL1 E1103G BH1L
G
YPD
YPRaf
YPRaf/Gal
SC-Leu
SC-Leu+MPA
SC-Lys
RPB1
rpb1-BH1
rpb1-TL1 E1103G BH1
rpb1-BH1L

Supplemental Data.

Figure S1. *In vitro* multiround transcription assay for Pol I, related to Figure 2

Activity of A190-E1224G and A190-F1205H Pol I complexes in multiround transcription assay. A) Promoter-dependent multiround transcription with purified components was performed exactly as described in (Bedwell et al., 2012). Yeast-derived pure Pol I (WT or mutant) was incubated with equi-molar concentrations of recombinant Rrn3 (Keener et al., 1998). The pre-initiation complex was assembled on the template (containing the rDNA promoter region and 336 nt of downstream DNA) using recombinant TBP and Core Factor, Upstream Activating Factor (UAF) purified from yeast, and pre-incubated Pol I-Rrn3. Transcription reactions were initiated with NTPs [200 μM of ATP, UTP and CTP, 15 μM of GTP and 10 μCi α-^{32}P-GTP (800 μCi/mmole)], incubated for 5 minutes and stopped by addition of excess phenol. RNA was ethanol precipitated, separated by 8% polyacrylamide gel electrophoresis and visualized by autoradiography. The runoff product is indicated by the *asterisk*. The reactions were performed in duplicate. Data shown are representative from one of three independent assays. **B)** Quantifications of the run-off product were done using Quantity One software, average values relative to the WT control from the three independent assays and the standard deviations are shown.

Figure S2. Quantification of *in vitro* pause intensity, related to Figure 2

Site specific pausing by A190-E1224G polymerase is enhanced *in vitro*. Three independent transcription elongation rate assays at low NTP concentrations were performed with WT and A190-E1224G Pol I (representative assay shown in Figure 2C). The major pause site intensity (indicated by an asterisk in Figure 2C) was quantified in each experiment and the values were normalized to intensity of halted elongation complexes at +56. The resulting values were plotted, with error bars = +/- 1 standard deviation.

Table S1. Total RNA synthesis rates of the *RPA190* and *rpa190-E1224G* strains, related to Table 1

Strain	Growth Rate (doublings/hr)	Total RNA, ng/μl	Predicted Synthesis Rate	Observed rRNA Synthesis Rate (from Figure S3 panel A)
WT	0.52	347.4	1	1
E1224G	0.51	288.3	0.82	0.94

Total RNA synthesis rates predicted for the *RPA190* and *rpa190-E1224G* strains. Since the rRNA synthesis rates measured by ^{3}H-methylmetionine incorporation pulse-and chase assay were done in SD-Met medium, we measured the total RNA synthesis rates and growth rates in SD-Met for a better

comparison. Total RNA was extracted from exponentially growing cells and measured spectrophotometrically (NanoDrop ND1000). The predicted synthesis rate was quantified as (**Growth Rate) X (Total RNA)** and normalized to WT. These data are representative from one experiment, qualitatively similar results were obtained from repeated analyses from independent cultures grown on different days.

Figure S3. The *rpa190-E1224G* mutant is not hyperactive *in vivo*, related to Figure 3

A) Relative Pol I transcription rates were measured using the [^{3}H]methylmethionine incorporation pulse-and-chase assay as described in (Zhang et al., 2010). Since rRNA is co-transcriptionally methylated, this method is an effective way to quantify rRNA synthesis *in vivo*. The cells were grown in SD-Met medium and pulse-labeled with [^{3}H]methylmethionine for 5 minutes, and then chased with excess cold methionine to allow completion of rRNA processing. RNA was extracted from cells collected 4 minutes after pulse and 5 minutes after chase (Zhang et al., 2010). The RNA species were separated by gel-electrophoresis, transferred to a membrane and detected by autoradiography. The lanes indicated as P ("pulsed") contain rRNA pulse-labeled for 4 min; and lanes C ("chased") contains 5 min pulse-labeled rRNA followed by a 5 minute chase. Data shown are from one of two independent experiments. **B)** Same as panel A, except the metabolic labeling was done using the *rrp6*Δ *RPA190 (WT)* or *rrp6*Δ *rpa190-E1224G* cells. Rrp6 is a non-essential subunit of the nuclear exosome involved in degradation of unstable precursors and defective rRNA (Allmang et al., 2000). The *rrp6*Δ *rpa190-E1224G* double mutant does not accumulate rRNA degradation intermediates, precursors, or mature rRNA species when compared to the single mutants. This experiment is an additional control for co-transcriptional exosome-dependent decay of rRNA.

C) Northern Blot analysis of the rRNA isolated from the *RPA190* and *rpa190-E1224G* strains. The Northern blot analysis was performed as described in (Schneider et al., 2007). Total RNA was extracted from exponentially growing cells; equal amount of RNA was loaded onto the 0.8% agarose gel in duplicates and separated by electrophoresis. After electrophoresis, RNA was transferred to a membrane and analyzed by northern blot hybridization using ^{32}P-labeled oligonucleotide probes (described in the Table S2). The blot was visualized using phosphorimaging (The Storm, GE Healthsciences). The rRNA species detected by the probes are indicated on the figure. No significant difference in the signal between the mutant and the WT was observed. Data shown are from one of the three independent experiments. **D)** The *rrp6*Δ and the *rrp6*Δ *rpa190-E1224G* cells were processed as described for panel C. No significant difference in the signal between the *rrp6*Δ and the double mutant was observed, supporting the rRNA

synthesis data (panels A and B). Data shown are from one of the two independent experiments. **E) The rDNA copy number of the *RPA190* and *rpa190-E1224G* strains** was determined based on the size of the chromosome XII separated from other yeast chromosomes using the Contour-clamped Homogenous Field Electrophoresis (CHEF) (as in (Zhang et al., 2009) and visualized with SYBR-Safe staining (Invitrogen, Carlsbad, CA). The migration distance of the chromosome XII of the reference strains (containing 190, 143, 42 and 25 rDNA copy numbers) was plotted versus the rDNA array size. The resulting linear plot (R^2=0.9916) yielded an equation [y=-33.2x+348.6] which was used to calculate rDNA copy number for the WT and *rpa190-E1224G* strains. We observed that the number of rDNA repeats in the mutant strain is not altered compared to WT. Since the number of the rDNA loci can potentially affect rRNA synthesis rate and rRNA abundance, this experiment was an additional control for the relative Pol I activity in *rpa190-E1224G.* **F) The Chromatin Immunoprecipitation (ChIP) analysis of Pol I occupancy over rDNA** was performed using polyclonal antibody against A190 subunit as described previously (Zhang et al., 2009). The bound DNA was measured using quantitative PCR and displayed as a ratio of precipitated to total DNA. The location of the primer sets used for the PCR on the rRNA gene is schematically depicted on the top of the panel. Each bar represents the average IP/input value for at least two 10-fold dilutions from at least two independent cultures. Error bars represent ± 1 SD. We observed no significant changes in Pol I occupancy of any region of the rDNA (promoter or throughout the coding region) relative to the WT control. Thus, given similar rRNA synthesis rates (panel A), and similar numbers of active genes (panel E and Figure 4), transcription initiation rates are approximately equal in the WT and mutant.

Table S2. Oligonucleotides used for the Northern Blot hybridization, related to Figures 3 and S3

Probe Target	Sequence	Reference
18S	5'-AGCCATTCGCAGTTTCACTG	this study
20S and 23S	5'-GCACAGAAATCTCTCACCGT	(Schneider *et al.*, 2007)
27S	5'-GCCTAGACGCTCTCTTCTTA	(Schneider *et al.*, 2007)
25S	5'-ACTAAGGCAATCCCGGTTGG	this study

Table S3. Summary of phenotypes observed in strains carrying chimeric alleles of *RPB1* (raw data shown in main text, Figure 4C)

Alleles	Phenotype				Interpretation
	Growth on YEPD	Suppression of *gal10Δ56*	Spt	MPA sensitivity	
RPB1	WT	not suppressed	Spt^+	Not MPA^s	WT
Common GOFs (e.g. E1103G)	N/A	weak or no suppression	Spt^-	MPA^s	GOF
Common LOFs (e.g. N479S)	N/A	strong suppression	Spt^+	MPA^r or not MPA^s	LOF
rpb1-TL1	Severe defect	strong suppression	Spt+	MPA^r	LOF
rpb1-TL1/E1103G	Mild defect	mild suppression	Spt+	Not MPA^s	E1103G suppresses *rpb1-TL1* growth phenotypes
rpb1-TL1X	Inviable				Inferred LOF
rpb1-TL1X/E1103G	Moderate defect	strong suppression	Spt^+	Not MPA^s	E1103G suppresses *rpb1-TL1X* inviability
rpb1-TL1/N479S	Inviable				Double mutant lethality
rpb1-TL1/E1103G/N479S	Severe defect	strong suppression	Spt^+	MPA^r	N479S suppresses growth suppression of *rpb1-TL1* by E1103G
rpb1-TL3	No defect	not suppressed	Spt^+	Not MPA^s	No obvious defect
rpb1-TL3/E1103G	Mild defect	weak suppression	Spt^+	Not MPA^s	E1103G slightly impairs *rpb1-TL3*
rpb1-TL3/N479S	No defect	weak suppression	Spt^+	Not MPA^s	N479S impairs *rpb1-TL3*
rpb1-TL3/E1103G/N479S	Mild defect	strong suppression	Spt^+	Not MPA^s	E1103G exacerbates effects of N479S on *rpb1-TL3*
rpb1-TL3X	Mild defect	not suppressed	Spt^+	Not MPA^s	Mild LOF

Figure S4. Chimeric alleles of *RPB1* accumulate excess Rpb1, but this is not the cause of chimera phenotypes; enzymes bearing the Pol I bridge helix and the Pol I trigger loop sequences do not mutually suppress impaired Pol II function, related to Figure 4

Chimeric alleles of *RPB1* accumulate excess Rpb1, but this is not the cause of chimera phenotypes; enzymes bearing the Pol I bridge helix and the Pol I trigger loop sequences do not mutually suppress impaired Pol II function, related to Figure 4. A) Western analysis for Rpb1 and Rpb3-TAP using anti-Rpb1 antibody (sc-25758, Santa Cruz Biotechnology) strains for WT and *rpb1-TL* chimera mutant strains. Extracts from equal cell equivalents and 1/3 said amount were subjected to SDS-PAGE,

immublotting and detection. Anti-Pgk1 (22C5D8, Life Technologies) blotting of same gel shown for loading control. **B)** Overexpression of Rpb1 via 2μ *RPB1* plasmid was analyzed relative to low copy CEN *RPB1* plasmid as in (A) for Rpb1, Rpb3-TAP, and Pgk1. **C)** Quantification of Western blotting using Bio-Rad Chemi-Doc system in conjunction with ImageQuant software (GE) shown in (A)(left graph, n≥4, average ratio Rpb1 signal/Rpb3-TAP signal ± standard deviation shown) or (B)(right graph same as left, n=3). **D)** Phenotypes of *rpb1-TL* chimera do not appear to derive from the Rpb1 overexpression observed in (A) for *rpb1-TL* mutant strains as the equal or greater overexpression observed in (B) does not result in phenotypes observed in Figure 4C. Very slight suppression of *gal10Δ56* is of a different quality from Pol II-Pol I/III chimeras and is much more similar to the appearance of papillae. These papillae may relate to *RPB1* being present in high copy, which may facilitate the genesis of dominant *rpb1* suppressors of *gal10Δ56*. **E)** Summary of chimeric *RPB1* bridge helix alleles used in this study. **F)** Plasmid shuffle results measuring viability of individual *rpb1* alleles. The assay is performed as described in the main text for Figure 5B. **G)** Dilutions of viable strains were plated on indicated growth media. Phenotypes were assessed as described in the main text for Figure 4C. *rpb1-BH1* did not show significant defects compared to WT. *rpb1-TL1/E1103G/BH1* suppressed *gal10Δ56* mutation and *rpb1-BH1L* was resistant to MPA: both phenotypes consistent with Pol II loss-of-function alleles.

Table S4. Strains used in this study, related to Figures 1-4

Table S5. Plasmids used in this study, related to Figures 1-4

pRS315	pBluescript, *CEN6, ARSH4, LEU2* (Sikorski and Hieter, 1989)
pRS316	pBluescript, *CEN6, ARSH4, URA3* (Sikorski and Hieter, 1989)
pRS315-*RPA190*	pRS315 derivative carrying wild type *RPA190*
pRS316-*RPA190*	pRS316 derivative carrying wild type *RPA190 (used for "plasmid shuffle" experiments)*
pRS306-*rpa190-E1224G*	pRS306 ("suicide vector") derivative carrying *rpa190-E1224G* used for the integration of *rpa190-E1224G* on the chromosome
pRS315-*rpa190-E1224G*	pRS315 derivatives carrying corresponding *rpa190* mutant alleles
pRS315-*rpa190-F1205H*	
pRS315-*rpa190-N1203S*	
pRS315-*rpa190-N1203S/E1224G*	
pRS315-*rpa190-H1206Y*	
pRS315-*rpa190-H1206Q*	
pRS315-*rpa190-H1206Q/E1224G*	
pRS315-*rpa190-F1207S*	
pRS315-*rpa190-F1207S/E1224G*	

pRS315-*rpa190-G1218D*	
pRS315-*rpa190-L1222S*	
pRS315-*rpa190-L1222S/E1224G*	
pCK plasmids:	pRS315 derivatives with corresponding *RPB1* alleles unless otherwise noted
pCK859	*RPB1* (Kaplan et al., 2012)
pCK960	*rpb1 E1103G* (Kaplan et al., 2012)
pCK856	*rpb1 N479S* (Kaplan et al., 2012)
pCK964	*rpb1 N479S/E1103G* (Kaplan et al., 2012)
pCK1143	pRS425 (2μ *LEU2*) derivative carrying *RPB1*
pCK1366	*rpb1-TL1/N479S*
pCK1367	*rpb1-TL1/E1103G/N479S*
pCK1368	*rpb1-TL1X/E1103G/N479S*
pCK1369	*rpb1-TL3/N479S*
pCK1371	*rpb1-TL1X/N479S*
pCK1372	*rpb1-TL1X BH1*
pCK1373	*rpb1-TL1X BH1L*
pCK1374	*rpb1-TL1 E1103G BH1*
pCK1375	*rpb1-TL1X E1103G BH1*
pCK1376	*rpb1-TL1 BH1L*
pCK1377	*rpb1-TL1 E1103G BH1L*
pCK1378	*rpb1-TL1*
pCK1379	*rpb1-TL1/E1103G*
pCK1380	*rpb1-TL3*
pCK1381	*rpb1-TL3/E1103G*
pCK1382	*rpb1-TL1X*
pCK1383	*rpb1-BH1L*
pCK1384	*rpb1-TL1 E1103G BH1*
pCK1385	*rpb1-TL1X/E1103G*
pCK1386	*rpb1-BH1*
pCK1387	*rpb1-TL1*
pCK1390	*rpb1-TL3*
pCK1393	*rpb1-TL3/E1103G*
pCK1394	*rpb1-TL3/E1103G/N479S*
pCK1395	*rpb1-TL1X E1103G BH1L*
pCK1397	*rpb1-TL3X*

Supplemental References

1. Allmang, C., Mitchell, P., Petfalski, E., and Tollervey, D. (2000). Degradation of ribosomal RNA precursors by the exosome. Nucleic acids research *28*, 1684-1691.
2. Bedwell, G.J., Appling, F.D., Anderson, S.J., and Schneider, D.A. (2012). Efficient transcription by RNA polymerase I using recombinant core factor. Gene *492*, 94-99.
3. Kaplan, C.D., Jin, H., Zhang, I.L., and Belyanin, A. (2012). Dissection of Pol II Trigger Loop Function and Pol II Activity-Dependent Control of Start Site Selection In Vivo. Plos Genet *8*.
4. Keener, J., Josaitis, C.A., Dodd, J.A., and Nomura, M. (1998). Reconstitution of yeast RNA polymerase I transcription in vitro from purified components. TATA-binding protein is not required for basal transcription. J Biol Chem. *273*, 33795-33802.

5. Schneider, D.A., Michel, A., Sikes, M.L., Vu, L., Dodd, J.A., Salgia, S., Osheim, Y.N., Beyer, A.L., and Nomura, M. (2007). Transcription elongation by RNA polymerase I is linked to efficient rRNA processing and ribosome assembly. Molecular cell *26*, 217-229.
6. Sikorski, R.S., and Hieter, P. (1989). A system of shuttle vectors and yeast host strains designed for efficient manipulation of DNA in Saccharomyces cerevisiae. Genetics *122*, 19-27.
7. Zhang, Y., Sikes, M.L., Beyer, A.L., and Schneider, D.A. (2009). The Paf1 complex is required for efficient transcription elongation by RNA polymerase I. Proceedings of the National Academy of Sciences of the United States of America *106*, 2153-2158.
8. Zhang, Y., Smith, A.D.t., Renfrow, M.B., and Schneider, D.A. (2010). The RNA polymerase-associated factor 1 complex (Paf1C) directly increases the elongation rate of RNA polymerase I and is required for efficient regulation of rRNA synthesis. The Journal of biological chemistry *285*, 14152-14159.

Strain	Description	Reference
DAS496 **(WT)**	*MATα ade2-1 ura3-1 trp1-1 leu2-3 112 his3-11,15 can1-100* ***RPA135-(HA)3-(His)7: TRP1 Mx6 rpa190Δ::HIS3Mx6*** **carrying** ***pRS315-RPA190***	this study
DAS702 **(E1224G)**	*MATα ade2-1 ura3-1 trp1-1 leu2-3 112 his3-11,15 can1-100* ***RPA135-(HA)3-(His)7: TRP1 Mx6 rpa190Δ::HIS3Mx6*** **carrying** ***pRS315-rpa190-E1224G***	this study
DAS701	*MATα ade2-1 ura3-1 trp1-1 leu2-3 112 his3-11,15 can1-100* ***rpa190-E1224G::LEU2Mx6***	this study
DAS715	same as DAS701, except *MAT* **a**	this study
DAS479	*MAT* **a** *ade2-1 ura3-1 trp1-1 leu2-3 112 his3-11,15 can1-100* ***rpa135-D784G: : neurseothricin-r***	this study
DAS703	*MAT* **a** *ade2-1 ura3-1 trp1-1 leu2-3 112 his3-11,15 can1-100* ***rpa49Δ::KANMx6***	this study
DAS531	*MAT* **a** *ade2-1 ura3-1 trp1-1 leu2-3 112 his3-11,15 can1-100* ***rpa12Δ:: URA4Mx6***	this study
DAS515	*MAT* **a** *ade2-1 ura3-1 trp1-1 leu2-3 112 his3-11,15 can1-100* ***paf1Δ::HIS3Mx6***	(Zhang et al., 2009)
DAS607	*MATα ade2-1 ura3-1 trp1-1 leu2-3 112 his3-11,15 can1-100* ***spt5(1-797) -(HA)*** $_3$ ***-(His)*** $_7$ ***:HIS3Mx6***	(Viktorovskaya et al., 2011)
NOY2167	*MAT* **a** *ade2-1 ura3-1 trp1-1 leu2-3 112 his3-11,15 can1-100* ***spt4Δ:HIS3Mx6***	(Schneider et al., 2006)
DAS704	*MAT* **a** *ade2-1 ura3-1 trp1-1 leu2-3 112 his3-11,15 can1-100* ***rrp6Δ::KANMx6***	this study
DAS206	*MATα ade2-1 ura3-1 trp1-1 leu2-3 112 his3-11,15 can1-100* ***trf4Δ: HIS3Mx6***	(Schneider et al., 2007)
NOY1075	*MAT* **a** *ade2-1 ura3-1 trp1-1 leu2-3 112 his3-11,15 can1-100* ***rrn3-S213P***	(Claypool et al., 2004)
DAS562	*MATα ade2-1 ura3-1 trp1-1 leu2-3 112 his3-11,15 can1-100* ***uaf30Δ::H IS3Mx6***	this study

DAS705	*MAT* **a**/*α* diploid resulted from cross DAS701 x DAS479	this study
DAS706	*MAT* **a**/*α* diploid resulted from cross DAS701 x DAS703	this study
DAS707	*MAT* **a**/*α* diploid resulted from cross DAS715 x DAS607	this study
DAS708	*MAT* **a**/*α* diploid resulted from cross DAS701 x DAS531	this study
DAS709	*MAT* **a**/*α* diploid resulted from cross DAS701 x DAS515	this study
DAS711	*MAT* **a**/*α* diploid resulted from cross DAS701 x NOY2167	this study
DAS710	*MAT* **a**/*α* diploid resulted from cross DAS715 x DAS206	this study
DAS712	*MAT* **a**/*α* diploid resulted from cross DAS702 x DAS704	this study
DAS713	*MAT* **a**/*α* diploid resulted from cross DAS701 x NOY1075	this study
DAS714	*MAT* **a**/*α* diploid resulted from cross DAS715 x DAS562	this study
DAS716 (***rrp6Δ*** **)**	*MATα ade2-1 ura3-1 trp1-1 leu2-3 112 his3-11,15 can1-100* ***rpa190Δ::HIS3Mx6 rrp6Δ::KANMx6*** **carrying** ***pRS315-RPA190***	this study
DAS717 (***rrp6Δ*** **E1224G)**	*MAT? ade2-1 ura3-1 trp1-1 leu2-3 112 his3-11,15 can1-100* ***rpa190Δ::HIS3Mx6 rrp6Δ::KANMx6*** **carrying** ***pRS315-rpa190-E1224G***	this study
NOY1071	*MATα ade2-1 ura3-1 trp1-1 leu2-3 112 his3-11,15 can1-100* ***fob1Δ::HIS3Mx6 rDNA copy number ~25***	(Cioci F, 2003)
NOY886	*MATα ade2-1 ura3-1 trp1-1 leu2-3 112 his3-11,15 can1-100* ***fob1Δ::HIS3Mx6 rpa135Δ::LEU2*** **with** ***pNOY117, rDNA copy number ~42***	(French et al., 2003)
NOY1051	same as NOY886, except ***rDNA copy number ~143***	(French et al., 2003)

NOY1064	same as NOY1071, except ***rDNA copy number ~190***	(Cioci F, 2003)
DAS721 **(F1205H)**	*MATα ade2-1 ura3-1 trp1-1 leu2-3 112 his3-11,15 can1-100* ***RPA135-(HA)3-(His)7: TRP1 Mx6 rpa190Δ::HIS3Mx6*** **carrying** ***pRS315-rpa190-F1205H***	this study
DAS764 **(L1222S)**	*MATα ade2-1 ura3-1 trp1-1 leu2-3 112 his3-11,15 can1-100* ***RPA135-(HA)3-(His)7: TRP1 Mx6 rpa190Δ::HIS3Mx6*** **carrying** ***pRS315-rpa190-L1222S***	this study
DAS765 **(N1203S/E1224G)**	*MATα ade2-1 ura3-1 trp1-1 leu2-3 112 his3-11,15 can1-100* ***RPA135-(HA)3-(His)7: TRP1 Mx6 rpa190Δ::HIS3Mx6*** **carrying** ***pRS315-rpa190- N1203S/E1224G***	this study
DAS766 **(F1207S)**	*MATα ade2-1 ura3-1 trp1-1 leu2-3 112 his3-11,15 can1-100* ***RPA135-(HA)3-(His)7: TRP1 Mx6 rpa190Δ::HIS3Mx6*** **carrying** ***pRS315-rpa190-F1207S***	this study
DAS767 **(F1207S/E1224G)**	*MATα ade2-1 ura3-1 trp1-1 leu2-3 112 his3-11,15 can1-100* ***RPA135-(HA)3-(His)7: TRP1 Mx6 rpa190Δ::HIS3Mx6*** **carrying** ***pRS315-rpa190-F1207S/E1224G***	this study
DAS768 **(H1206Q)**	*MATα ade2-1 ura3-1 trp1-1 leu2-3 112 his3-11,15 can1-100* ***RPA135-(HA)3-(His)7: TRP1 Mx6 rpa190Δ::HIS3Mx6*** **carrying** ***pRS315-rpa190-H1206Q***	this study
DAS769 **(H1206Q/E1224G)**	*MATα ade2-1 ura3-1 trp1-1 leu2-3 112 his3-11,15 can1-100* ***RPA135-(HA)3-(His)7: TRP1 Mx6 rpa190Δ::HIS3Mx6*** **carrying** ***pRS315-rpa190-H1206Q/E1224G***	this study
DAS770	*MATα ade2-1 ura3-1 trp1-1 leu2-3 112 his3-11,15 can1-100* ***RPA135-(HA)3-(His)7: TRP1 Mx6 rpa190Δ::HIS3Mx6*** **carrying** ***pRS316-RPA190*** **and** ***pRS315-rpa190-***	this study
DAS771	*MATα ade2-1 ura3-1 trp1-1 leu2-3 112 his3-11,15 can1-100* ***RPA135-(HA)3-(His)7: TRP1 Mx6 rpa190Δ::HIS3Mx6*** **carrying** ***pRS316-RPA190*** **and** ***pRS315-rpa190-***	this study
DAS772	*MATα ade2-1 ura3-1 trp1-1 leu2-3 112 his3-11,15 can1-100* ***RPA135-(HA)3-(His)7: TRP1 Mx6 rpa190Δ::HIS3Mx6*** **carrying** ***pRS316-RPA190*** **and** ***pRS315-rpa190-***	this study
DAS773	*MATα ade2-1 ura3-1 trp1-1 leu2-3 112 his3-11,15 can1-100* ***RPA135-(HA)3-(His)7: TRP1 Mx6 rpa190Δ::HIS3Mx6*** **carrying** ***pRS316-RPA190*** **and** ***pRS315-rpa190-***	this study
CKY283	*MATa ura3-52 his3Δ200 leu2Δ1 or Δ0 trp1Δ63 met15Δ0 lys2-128∂ gal10Δ56 rpb1Δ::CLONATMX RPB3::TAP::KlacTRP1 [pRP112 RPB1 URA3 CEN]*	(Kaplan et al., 2008)
CKY1271	*MATa ura3-52 his3Δ200 leu2Δ1 or Δ0 trp1Δ63 met15Δ0 lys2-128∂ gal10Δ56 rpb1Δ::CLONATMX RPB3::TAP::KlacTRP1 [rpb1-TL1/E1103G/N479S LEU2 CEN]* further referred as to CKY283 derivative carrying pCK1367	this study
CKY1272	CKY283 derivative carrying pCK1369	this study

CKY1273	CKY283 derivative carrying pCK1374	this study
CKY1274	CKY283 derivative carrying pCK1378	this study
CKY1275	CKY283 derivative carrying pCK1379	this study
CKY1276	CKY283 derivative carrying pCK1380	this study
CKY1277	CKY283 derivative carrying pCK1383	this study
CKY1278	CKY283 derivative carrying pCK1384	this study
CKY1279	CKY283 derivative carrying pCK1385	this study
CKY1280	CKY283 derivative carrying pCK1386	this study
CKY1281	CKY283 derivative carrying pCK1387	this study
CKY1282	CKY283 derivative carrying pCK1391	this study
CKY1283	CKY283 derivative carrying pCK1393	this study
CKY1284	CKY283 derivative carrying pCK1394	this study
CKY1285	CKY283 derivative carrying pCK859	this study
CKY1286	CKY283 derivative carrying pCK960	this study
CKY1287	CKY283 derivative carrying pCK856	this study
CKY1288	CKY283 derivative carrying pCK964	this study
CKY1340	CKY283 derivative carrying pCK1143	this study